Project 2 Report

Se Hwan Jeon

March 6, 2020

1 Human Arm Model

A planar model of the human arm was developed from the structure of the vertical model used by Ogihara and Yamazaki, shown in Figure 1 [1]. As the position of the wrist was moved in an elliptical path, the velocities, joint torques, and active muscle forces were determined from empirically determined models of motor control.

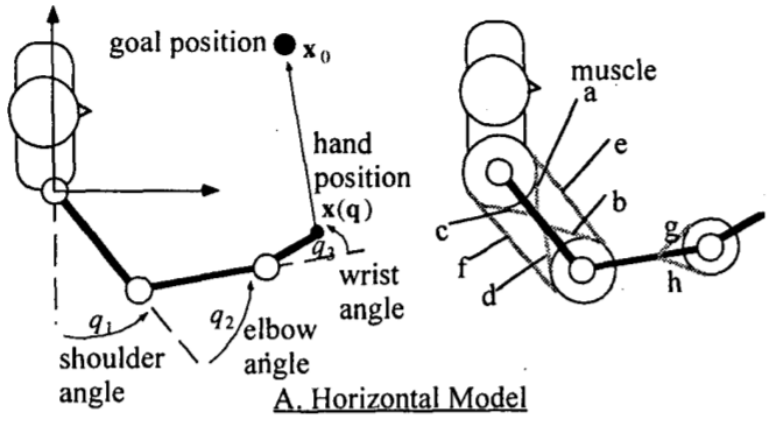

Figure 1: Horizontal model of human arm complex. $a - h$ represent muscles acting on the links of the arm. The corresponding muscles for $a - h$ is detailed in Appendix A [1].

1.1 Assumptions

A number of assumptions were made to perform the analysis described.

- All motion is solely parallel to the horizontal plane, and so the effect of gravity will be ignored.
- The human arm consists of three rigid links consisting of the upper arm, forearm, and wrist.
- The analysis will not consider the flexion of the wrist, and the angle q_3 in Figure 1 will equal 0° for all configurations and the forces applied from g and h will be ignored.
- The moment arms of the engaged muscles were assumed to be constant for all configuration positions.
- Only the defined muscles $a - h$ in Figure 1 control the movement of the arm, and act as pure force generators.
- The path is independent of the required muscle forces.
- The system will be analyzed at constant steady-state tracing of the elliptical path.
- The length-tension and velocity-tension relationships for muscles will be ignored.
- There is no change in physiological cross-sectional area (PCSA) of the muscles.

2 System State Space

2.1 Ellipse Tracing

The model shown in Figure 1 was modified to determine the joint angles of the shoulder and elbow as a function of the ellipse angle, as shown in Figure 2. The center of the ellipse was defined as some (x_c, y_c), with a semi-major and semi-minor axis of a and b respectively. The parametric equations for an ellipse can be given as

$$a\cos(\phi) + x_c = x, \tag{2.1}$$

$$b\sin(\phi) + y_c = y, \tag{2.2}$$

where x and y are the coordinates of the points on the elliptical path.

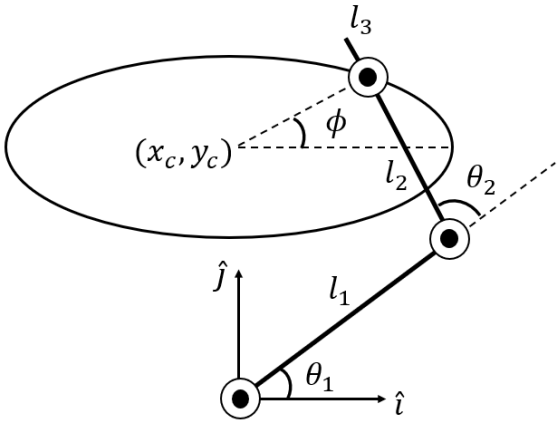

Figure 2: Developed model of human arm complex.

To ensure all positions in the path were possible, the considered ellipse would need to be within the workspace of the considered segment. The position of the wrist when the arm was fully retracted and extended determined the limits of the workspace. An appropriate position and axis lengths chosen for the ellipse was $x_c = 0.05$ m, $y_c = 0.35$ m, $a = 0.35$ m, and $b = 0.10$ m. The path was plotted over the workspace of the arm to ensure solutions would exist for the arm configurations, as shown in Figure 3.

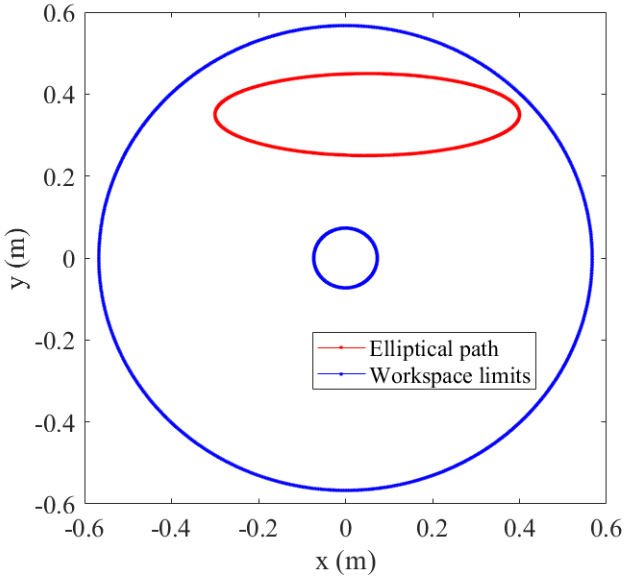

Figure 3: Defined elliptical path with workspace limits.

From the defined system in Figure 2, equations for the vertical and horizontal position of the wrist could be defined as a function of θ_1 (shoulder angle), θ_2 (relative elbow angle), and ϕ (ellipse angle), given below as

$$x_w = l_1 \cos(\theta_1) + l_2 \cos(\theta_1 + \theta_2) = x_c + a\cos(\phi), \tag{2.3}$$

$$y_w = l_1 \sin(\theta_1) + l_2 \sin(\theta_1 + \theta_2) = y_c + b\sin(\phi), \tag{2.4}$$

where x_w and y_w are the horizontal and vertical position of the wrist with respect to the origin (the shoulder joint).

Using MATLAB's `vpasolve` command, Equations 2.3 and 2.4 were numerically solved for θ_1 and θ_2 as ϕ was varied from 0° to 360° with 1000 points. By limiting the range of solutions to be between 0° and 360° for θ_1 and 0° and 180° for θ_2, it was ensured the "elbow out" solution would be found for each configuration of ϕ. The plot of joint angle against ϕ is shown in Figure 4.

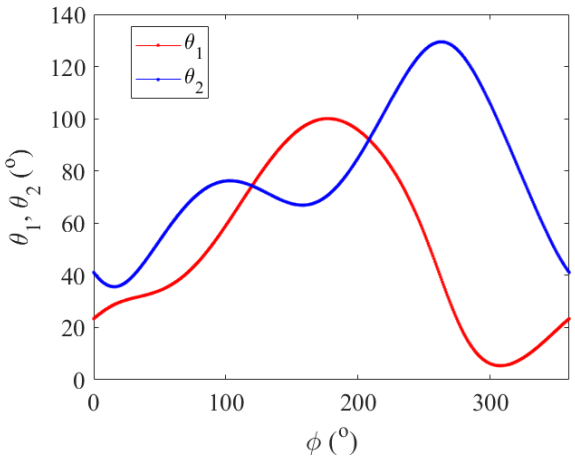

Figure 4: Joint angle evolution as ϕ is changed.

2.2 Tangential Velocities

The determine the tangential velocities at each point along the ellipse, the 2/3 Power Law was used [2], and is given as

$$v_T = k(\rho)^{\frac{1}{3}}, \tag{2.5}$$

where v_T is the tangential velocity, k is a gain parameter, and ρ is the radius of curvature of the path. For the defined elliptical path, the curvature κ, defined as the reciprocal of the radius, can be found to be

$$\kappa = \frac{ab}{(a^2 \sin^2 \phi + b^2 \cos^2 \phi)^{\frac{3}{2}}}. \tag{2.6}$$

A "typical", fast, and slow case were considered for the ellipse tracing task. The gain values were $k = 15$, 30, and 50 respectively. To find the total time taken by each of these cases, the the arclength of the ellipse segment that two points were divided by the tangential velocity averaged at those two points to find the local time step. The arclength of an ellipse between values of ϕ can be evaluated numerically from the incomplete elliptical integral of the second kind, given as

$$L = \int_0^{\phi} \sqrt{1 - e^2 \sin^2 \phi} \mathrm{d}\phi, \tag{2.7}$$

where e is the eccentricity of the ellipse, given as $e^2 = 1 - \frac{b^2}{a^2}$, and L is the length of the curve [3]. Fortunately, MATLAB has a built in function that evaluates incomplete elliptical integrals of the second kind, and so the `ellipticE` command was used to find the arclengths and subsequent time steps between each point.

These local time steps were summed over all the points on the ellipse to determine the total time taken to trace the path, and were found to be 9.26, 4.63, and 2.78 seconds for the slow, typical, and fast cases respectively. The tangential velocities were plotted as a function of ϕ, and is shown in Figure 5.

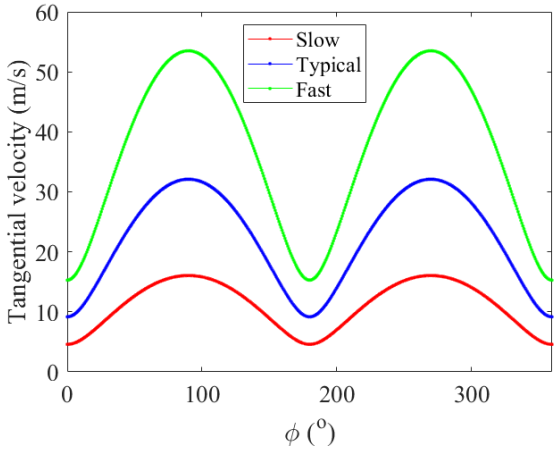

Figure 5: Tangential velocities for slow, typical, and fast cases as a function of ϕ.

As Equation 2.5 suggests, the tighter the traced curve, the slower the absolute velocity of the wrist. While this behaviour tends to break down for straight movements (where $\rho = \infty$, this 2/3 power relation has held true for a subset of motor tasks that suggest at a more general relationship between joint speed and curvature.

3 Task Tolerance

Although the path is elliptical rather than straight, the average tolerances of the fast and slow cases can be compared to the typical case by using Fitts's Law, given as

$$ID = -\log_2(\frac{W_s}{2A}), \tag{3.1}$$

$$IP = \frac{ID}{t}, \tag{3.2}$$

where ID is the binary index of difficulty, W_s is the average tolerance, A is the amplitude of the task, IP is the binary index of performance, and t is the total time taken for the task [4]. Fitts's Law theorizes that IP is generally constant for each individual, and that the difficulty of the task can be evaluated as a function of the tolerance required, the speed at which it is performed, and the amplitude of the task.

In this case, the average amplitude of each case is the same, as they all trace the same ellipse. Equations 3.1 and 3.2 can be combined and re-expressed as

$$W_{s,i} = A(2^{1-IP(t_i)}), \tag{3.3}$$

where $W_{s,i}$ is the average tolerance of case i, and t_i is the time taken by case i. By dividing the average tolerance of the fast and slow cases by that of the typical case, the IP and A terms are eliminated, and the ratio can be expressed as

$$\frac{W_{s,i}}{W_{s,typical}} = 2^{t_{typical}-t_i}. \tag{3.4}$$

With the total times for the cases determined previously, the average tolerance for the slow speed is 4.04% of that of the typical case, and the average tolerance for the fast speed is 361% that of the typical case. As the time taken for the task is varied, the tolerance for the

task is affected significantly. As intuition suggests, the slower the task the more precisely it can be done, and vice versa.

4 Joint Speed Ratios

4.1 Joint Velocities

To determine the joint velocities of the arm model, the following relation was used:

$$\begin{bmatrix} \dot{x} \\ \dot{y} \end{bmatrix} = \boldsymbol{J} \begin{bmatrix} \dot{\theta_2} \\ \dot{\theta_1} \end{bmatrix}, \tag{4.1}$$

where $\boldsymbol{J}$ is the Jacobian matrix derived from Equations 2.3 and 2.4, and is given as

$$\boldsymbol{J} = \begin{bmatrix} -l_2 \sin(\theta_1 + \theta_2) & -l_2 \sin(\theta_1 + \theta_2) - l_1 \sin(\theta_1) \\ l_2 \cos(\theta_1 + \theta_2) & l_2 \cos(\theta_1 + \theta_2) + l_1 \cos(\theta_1). \end{bmatrix}. \tag{4.2}$$

For each of the three speed cases, the Cartesian velocity components can be found as

$$\begin{bmatrix} \dot{x} \\ \dot{y} \end{bmatrix} = \begin{bmatrix} v_T \cos(\phi) \\ v_T \sin(\phi) \end{bmatrix}. \tag{4.3}$$

By taking the inverse of the Jacobian and multiplying it with Equation 4.3, the joint velocities of the speed was calculated for each value of ϕ for each of the three cases. By dividing $\dot{\theta_2}$ by $\dot{\theta_1}$, the instantaneous joint velocities were plotted as a function of ϕ, as shown in Figure 6.

Regardless of the speed at which the elliptical tracing task was performed, the relative speed ratios between the elbow and shoulder joint seem the same. Furthermore, it seems singularities exist in the motion of the system. There appear to be points where the joint velocity of the shoulder is near 0, creating the sharp peaks observed near 260° and 340°. As can also be observed in robotic limbs, these singularity points are regions where large angle changes are required for relatively small changes in the position of the tool frame, and, for the elliptical path defined, there appear to be at least two such points in the motion of the wrist.

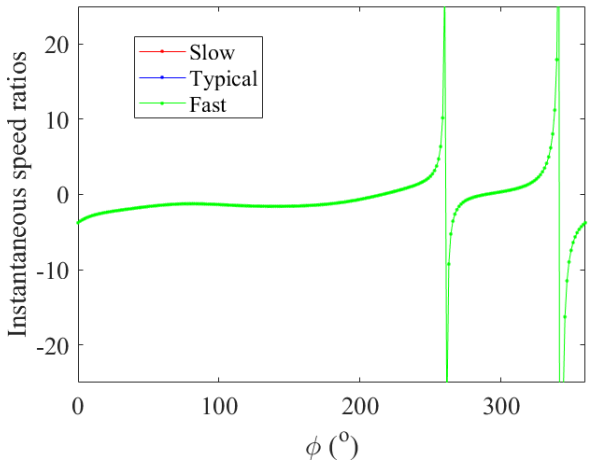

Figure 6: Joint ratios for slow, typical, and fast cases for elliptical tracing. Note that all curves overlap.

5 Joint Torques

5.1 Individual Joint Torques

For the slow, typical, and fast cases of the elliptical tracing motion, the shoulder and elbow joint torques were calculated. From the work of Dounskaia et al. [5], the torque at these joints can be expressed as

$$T_e = I_e\ddot{\theta}_2 + (I_e + r_e l_1 m_2 \cos(\theta_2))\ddot{\theta}_1 + r_e l_1 m_2 \sin(\theta_2)\dot{\theta}_1^{\,2}, \tag{5.1}$$

$$\begin{aligned} T_s = {} & I_s\ddot{\theta}_1 + \left[I_e + m_2(l_1^2 + 2r_e l_1 \cos(\theta_2))\right]\ddot{\theta}_1 + (I_e + r_e l_1 m_2 \cos(\theta_2))\ddot{\theta}_2 \\ & -r_e l_1 m_2 \sin(\theta_2)\dot{\theta}_2^{\,2} - 2r_e l_1 m_2 \sin(\theta_2)\dot{\theta}_1\dot{\theta}_2, \end{aligned} \tag{5.2}$$

where I_e and I_s are the mass moments of inertia about the axis of rotation for the elbow and shoulder respectively, r_e is the proximal distance between the elbow joint and the center of mass of the forearm, and m_e is the mass of the lower arm (forearm and hand).

The constant parameters of the system can be found in Appendix A [1]. Note that the given values of inertia are for the center of mass, and were adjusted with the parallel axis theorem to be for hte proximal end as Equation 5.1 and 5.2 requires. With the joint velocities calcu-

lated previously, the `gradient` function was used in MATLAB to obtain the accelerations at each position along the ellipse. The function uses a finite first-order central difference scheme to evaluate the numerical derivative for a given vector of points. MATLAB was used to numerically evaluate the shoulder and elbow torques at each position of ϕ

The torque at the shoulder and elbow were plotted for each value of ϕ along the elliptical path for each case, and is shown in Figure 7.

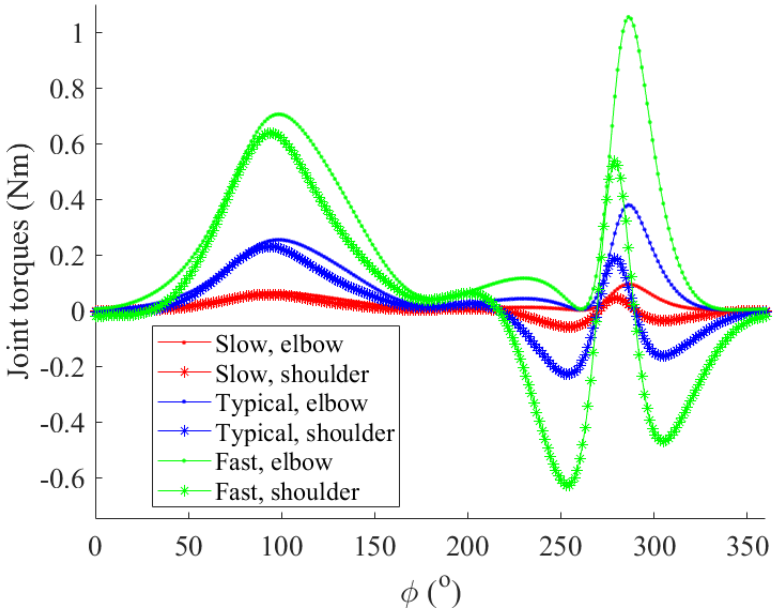

Figure 7: Joint torques for slow, typical, and fast cases.

While the joint torques are largely a function of the arm's position along the elliptical path, there is a general trend of torque increasing as the movement gets faster. More significantly, the relative torque ratio between the shoulder and elbow becomes more exaggerated as the movement becomes faster as well. It seems that for certain regions, either the elbow or shoulder torque seems dominant, but for others, they remain approximately the same. There are also regions where the torque is negative, which are most likely because the arm requires a significant amount of deceleration as it approaches tighter radii of curvature. These results seems similar to other studies done concerning the shoulder and elbow torques in point-to-point reaching motions, as well as the leading joint hypothesis [5, 6]. However, there appear to be significant interaction torques between the shoulder and elbow that cannot be ignored.

5.2 Scaled Joint Torques

The joint torques for the cases were also estimated by using Hollerbach's dynamic scaling equations [7], given by the relation

$$\tau' = c^2\tau, \tag{5.3}$$

where c is the time scaling constant, τ' is the vector of scaled torques, and τ is the vector of original torques. c was determined by dividing the total times taken to trace the ellipse for each case. The joint torques for three scaled cases were considered:

- The joint torques for the typical and fast trajectories, scaled from the slow trajectory.
- The joint torques for the slow and fast trajectories, scaled from the typical trajectory.
- The joint torques for the typical and slow trajectories, scaled from the fast trajectory.

Figure 8, 9, and 10 shows the plots of the joint torques for these cases respectively. The scaled joint torques are plotted alongside the difference between the torques obtained from Figure 7 and the scaled estimate of those torques.

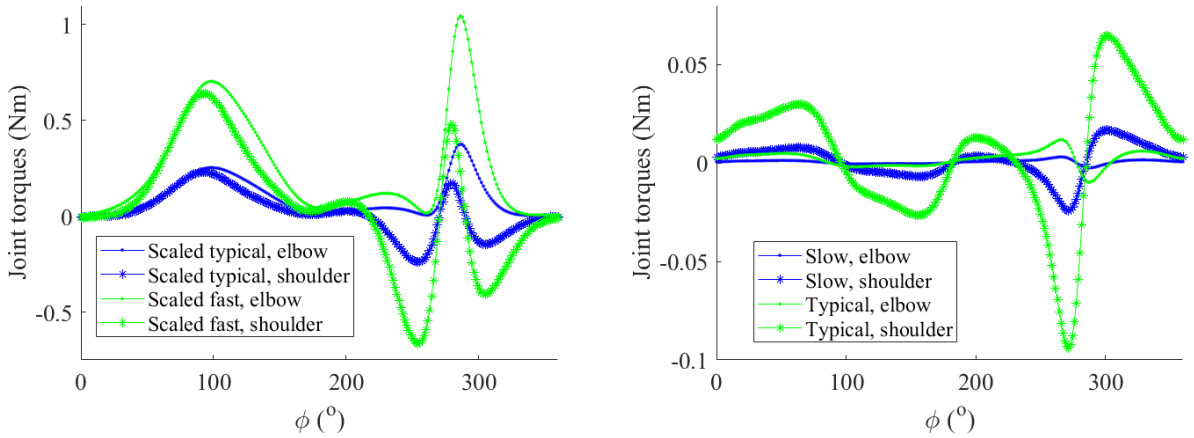

Figure 8: Joint torques for typical and fast cases, scaled from slow speed (left), and difference between scaled and calculated torques (right).

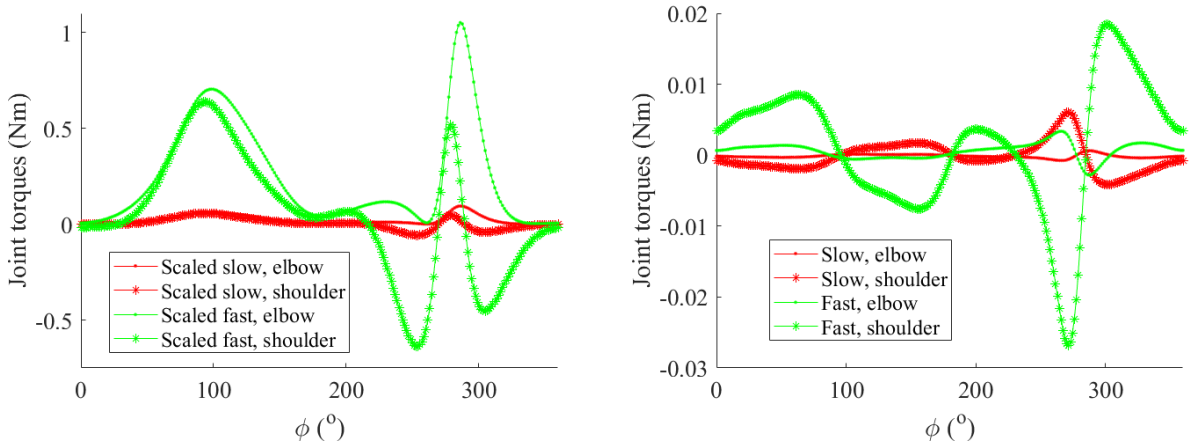

Figure 9: Joint torques for slow and fast cases, scaled from typical speed (left), and difference between scaled and calculated torques (right).

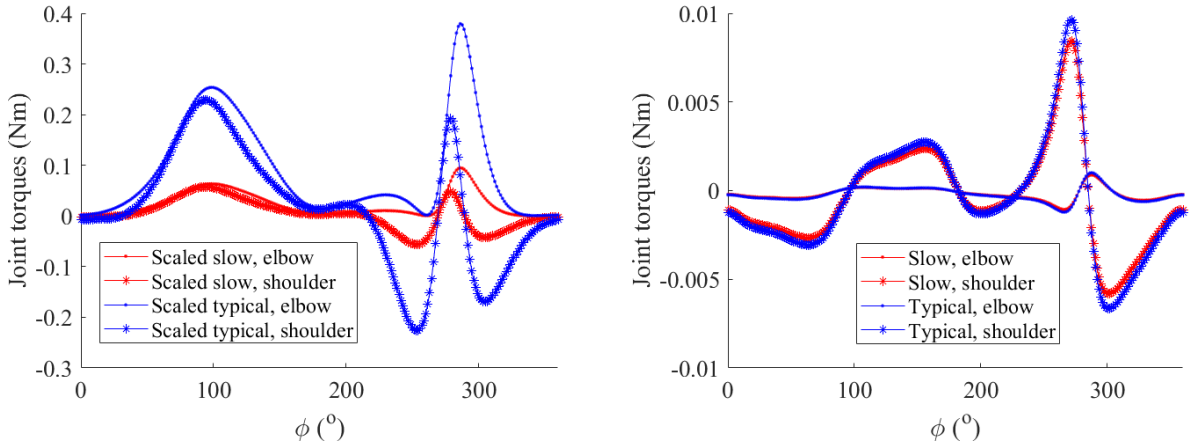

Figure 10: Joint torques for typical and slow cases, scaled from fast speed (left), and difference between scaled and calculated torques (right).

Generally, the joint torques predicted by Hollerbach's dynamic scaling equations seems very close to those calculated directly with Equations 5.1 and 5.2. The magnitude of the difference does not exceed 0.1 N/m. Comparing Figures 8 and 10, it seems that scaling to a higher speed from a slower speed is generally more inaccurate than the other way around. Physically, it is similarly easier to execute a motion slower than how it was learned than to speed it up and maintain the same level of precision.

6 Muscle Force Optimization

The muscles acting on the joints in Figure 1 were assumed to be pure force generators, and to achieve the torques from the calculated fast trajectory and fast trajectory scaled from the typical speed, the total muscle activation was minimized to determine an optimal solution to the forces required. The activation can be expressed as

$$f_1(\mathbf{F}) = \sum_{i=a}^{i=f} \frac{F_i}{F_{i,max}}, \tag{6.1}$$

where f_1 is the objective function, F_i is the force of the muscle, and $F_{i,max}$ is the maximum force of that specific muscle, shown in Appendix A [1].

For the cases, the following constraints and bounds were defined to be used with MATLAB's `fmincon` function.

$$\mathbf{F} \leq \mathbf{F_{max}}, \tag{6.2}$$

$$\mathbf{T} = \mathbf{GF}, \tag{6.3}$$

$$\mathbf{F} \geq \mathbf{0}, \tag{6.4}$$

where $\mathbf{F_{max}}$ is a vector of the maximum forces for each of the muscles. The default initial guess of 0 for all muscle activations was used, as the activation was required to be positive and less than 1. The plots of the muscle forces vs. ϕ are shown in Figure 11 below.

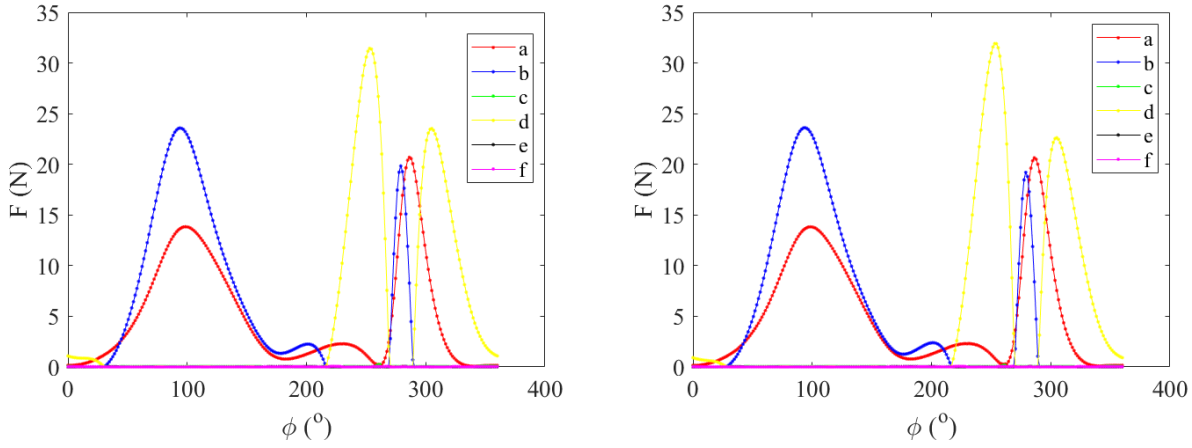

Figure 11: Optimized muscle forces for calculated torque with fast trajectory (left) and optimized forces for fast trajectory scaled from typical trajectory (right).

7 Discussion

Both optimized muscle force plots appear similar, which is to be expected, as the torques required from both the fast trajectory, and the fast trajectory scaled from the typical case are likewise similar, as can be seen in Figure 9. In order to minimize the required optimization, it can be seen that no antagonistic muscle pairs (a-c, b-d, etc.) are ever active at the same time. Furthermore, it seems that both biarticular muscles, e and f, and the major latissimus dorsi, muscle c, are never activated. The elliptical tracing task is accomplished purely by contracting the shoulder muscle with no extension required.

Because the biarticular muscles have a smaller maximum force, their activation would increase faster than that of the other muscles, explaining why neither are used at all in Figure 11. It is possible that if a different objective function, such as total force, were minimized instead, these biarticular muscle forces may be present.

As can be seen from Figure 6, regions of the traced path where the elbow joint angle velocity is large correspond to large forces in the muscles controlling the elbow. Furthermore, to decelerate and accelerate the forearm, a sharp rise in muscle d follows the drop in force from muscle a and b that match the 2/3 Power Law. Generally speaking, there appears to be a positive correlation between the magnitude of the joint torque, joint velocity, and magnitude of the applied muscle force from the results shown.

References

[1] Ogihara, N., and Yamazaki, N., 1999, "Generation of human reaching movement using a recurrent neural network model," In Proceedings of IEEE International Conference on Systems, Man, and Cybernetics, 2, pp. 692 - 697.

[2] Viviani, P., and Schneider, R., 1991, "A developmental study of the relationship between geometry and kinematics in drawing movements," J Exp Psychol Hum Percept Perform. 17(1):198-218.

[3] Abbott, P. (2009). On the Perimeter of an Ellipse. The Mathematica Journal, 11(2). doi: 10.3888/tmj.11.2-4

[4] Fitts, P.M. (1954). The information capacity of the human motor system in controlling the amplitude of movement. Journal of Experimental Psychology, volume 47, number 6, pp. 381–391.

[5] N. Dounskaia. The internal model and the leading joint hypothesis: implications for control of multi-joint movements. Experimental Brain Research, 166:1-16, 2005.

[6] S. Ambike J.P. Schmiedeler. The leading joint hypothesis for spatial reaching arm motions. Experimental Brain Research, 224(4):591-603, 2013.

[7] J.M. Hollerbach. Dynamic scaling of manipulator trajectories. ASME Journal of Dynamic Systems, Measurement, and Control, 106:102-106, 1984.

Appendix A: Muscle Parameters

	Max Force[N]	MA[m]	
a. M. pectoralis major	840	-0.051(s)	
b. M. brachialis	560	-0.027(e)	
c. M. latissimus dorsi	800	0.041(s)	
d. M. triceps brachii breve	480	0.020(e)	
e. M. biceps brachii	200	-0.029(s)	-0.043(e)
f. M. triceps brachii longue	240	0.025(s)	0.023(e)
g. M. flexor carpi rad & ulna	141	-0.017(w)	
h. M. ext carpi rad & ulna	144	0.019(w)	

Note: MA=moment arm, (s), (e) and (w) denote MA around shoulder, elbow, and wrist joints, respecitively.

Figure 12: Muscle designations, forces, and moment arms [1].

	mass[kg]	length[m]	C.G[m]	Inertia[kgm^2]
Upper arm	1.68	0.320	0.141	0.0133
Fore arm	0.96	0.247	0.106	0.0067
Hand	0.36	0.184	0.094	0.0006

Figure 13: Inertial and geometric parameters of upper arm, forearm, and hand [1].